



LAWRENCE
LIVERMORE
NATIONAL
LABORATORY

LLNL-PROC-717402

Energy Evolution of the Fission-Product Yields from Neutron-Induced Fission of ^{235}U , ^{238}U , and ^{239}Pu : An Unexpected Observation

A. Tonchev, M. Stoyer, J. Becker, R. Macri, C. Ryan, S. Sheets, M. Gooden , C. Arnold, E. Bond, T. Bredeweg, M. Fowler, G. Rusev, D. Vieira, J. Wilhelmy, W. Tornow , C. Howell, C. Bhatia , M. Bhike, F. Krishichayan, J. Kelley, B. Fallin , S. Finch

January 10, 2017

The 6th International Conference on "Fission and Properties of Neutron-Rich Nuclei" (ICFN6)
Sanibel Island, FL, United States
November 6, 2016 through November 12, 2016

Disclaimer

This document was prepared as an account of work sponsored by an agency of the United States government. Neither the United States government nor Lawrence Livermore National Security, LLC, nor any of their employees makes any warranty, expressed or implied, or assumes any legal liability or responsibility for the accuracy, completeness, or usefulness of any information, apparatus, product, or process disclosed, or represents that its use would not infringe privately owned rights. Reference herein to any specific commercial product, process, or service by trade name, trademark, manufacturer, or otherwise does not necessarily constitute or imply its endorsement, recommendation, or favoring by the United States government or Lawrence Livermore National Security, LLC. The views and opinions of authors expressed herein do not necessarily state or reflect those of the United States government or Lawrence Livermore National Security, LLC, and shall not be used for advertising or product endorsement purposes.

**Energy Evolution of the Fission-Product Yields from
Neutron-Induced Fission of ^{235}U , ^{238}U , and ^{239}Pu :
An Unexpected Observation**

A.P. Tonchev*, M.A. Stoyer, J.A. Becker, R. Macri, C. Ryan, S.A. Sheets

Lawrence Livermore National Laboratory, Livermore, California 94550, USA

**E-mail: tonchev2@llnl.gov*

M.E. Gooden, C. Arnold, E. Bond, T. Bredeweg, M.M. Fowler, G. Rusev, D.J. Vieira,
J.B. Wilhelmy

Los Alamos National Laboratory, Los Alamos, New Mexico 87545, USA

W. Tornow^{1,2}, C.H. Howell^{1,2}, C. Bhatia^{1,2}, M. Bhike^{1,2}, Krishichayan^{1,2}, J.H.
Kelley^{1,3}, B. Fallin^{1,2}, S. Finch^{1,2}

¹ Triangle Universities Nuclear Laboratory, Durham, North Carolina 27708, USA

² Department of Physics, Duke University, Durham, North Carolina 27708, USA

*³ Department of Physics, North Carolina State University, Raleigh, North Carolina
27605, USA*

A consistent set of high-precision measurements have been performed to study the energy dependence of the fission product yields of ^{235}U , ^{238}U , and ^{239}Pu using monoenergetic neutrons between 0.5 and 14.8 MeV. The results confirm the progression towards symmetric fission at higher incident neutron energy, i.e. 14.8 MeV. However at lower energies ($E_n < \sim 3$ MeV) the experimental data reveal a peculiar energy dependence of some high-yield fission fragments from neutron-induced fission of ^{239}Pu : a positive slope up to about 4–5 MeV which then turns negative as the incident neutron energy increases. This latter finding at low-energy is in conflict with present theoretical predictions.

Keywords: neutron-induced fission; fission product yields; fission ionization chambers, gamma-ray spectroscopy; quasi-monoenergetic neutron beams;

1. Introduction

Nuclear fission, the most pronounced collective nuclear-structure phenomenon, relates the fission product yields and their kinetic energies to the potential energy of the fissioning system¹. The evolution of the fis-

sioning system from the initial particle impact through intermediate saddle points to scission and finally to the configuration of separated fission fragments is governed by multi-dimensional potential-energy surfaces and the shell structure of the fragments. At low excitation energies shell and pairing effects in nuclei influence both the mass and energy distribution of the fission fragments. Hence, fine nuclear structure details are needed to describe experimental fission data. At higher excitation energies well above the barrier, shell and pairing effects become washed out and fission is well described by a liquid drop model. Therefore, only at low excitation energies, close to the fission barrier, do subtle effects show up when the excitation energy is varied. These variations are intimately connected with changes in the mass distributions which furthermore are affected by variations of the spin of the compound nuclear system. Models, based on different phenomenological and microscopic approaches are used to describe the complexity of the fission process and are gauged on how well they describe the various experimental observables². One of these observables is dependence on incident neutron energy of the Fission Product Yields (FPYs). The magnitude and the slope of the energy dependencies of the FPYs have significant impact on basic and applied physics³⁻⁶. For example, r-process nucleosynthesis cannot be fully understood without a precise knowledge of the fission properties of the very neutron-rich isotopes of the heaviest elements, which are presently not accessible to direct measurements. Precise knowledge of FPYs are important for nuclear reactors, nondestructive nuclear fuel investigation, accelerator-driven systems, and decay heat. In addition, information on the FPYs has a fundamental impact on basic fission studies and antineutrino spectrum⁷. The accuracy of purely theoretical predictions is insufficient for quantitative predictions of the energy dependence of fission yields with the precision that present nuclear applications require¹¹. However, it is quite challenging to make quantitative predictions of the FPYs, especially within a microscopic approach based on time-dependent Hartree-Fock calculations, where the experimental magnitude of the energy dependence is comparable or even smaller than the uncertainties of the theoretically calculated FPYs^{10,12}.

This paper reveals the energy evolution of the fission-product yields from neutron-induced fission of ^{235}U , ^{238}U , and ^{239}Pu using quasi-monoenergetic neutrons. The main experimental results of this study have been published in Refs. ¹³⁻¹⁵.

2. Experimental Overview

The FPY measurements were performed employing the 10 MV Van der Graaff Tandem accelerator at the Triangle Universities Nuclear Laboratory (TUNL). Monoenergetic neutrons were produced via utilizing four nuclear reactions $^7\text{Li}(p, n)^7\text{Be}$, $^3\text{H}(p, n)^3\text{He}$, $^2\text{H}(d, n)^3\text{He}$, and $^3\text{H}(d, n)^4\text{He}$, providing high yield of fast neutrons^{13,15}. These reactions cover different energy ranges in which the produced neutrons are truly monoenergetic and the contribution from off-energy neutrons are negligible¹⁶. A schematic of the experimental setup is shown in Fig. 1. The incident deuteron or proton beam passes through a $6.5\ \mu\text{m}$ Havar foil, enters a helium buffer cell and after traversing a tritium loaded layer of titanium is finally stopped in a thin copper beam stop. At different irradiation configuration the tritiated target can be replaced by either ^7Li target or ^2H gas cell allowing to produce quasi-monoenergetic neutrons with different energies.

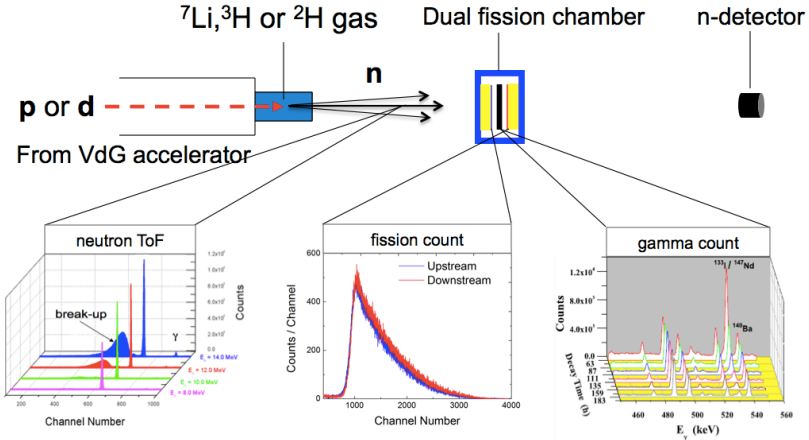


Fig. 1. Schematic of the FPY experimental setup at TUNL. A dual-fission chamber is positioned 4 cm downstream from the neutron production source while a liquid-scintillator neutron detector is positioned 3 m downstream neutron production and served as a secondary flux monitor.

A dual-fission chamber (DFC) chamber is used to provide the most accurate determination of the total number of fissions during the irradiation. The DFC is located in close proximity (4 cm) to the neutron production source. The chamber contains two thin reference foils and a thicker actinide activation target¹⁶. The activation target is contained in the center

of the chamber while the thin reference foils are up- and down-stream from the activation target in identical ionization chambers. The thick activation target is of the same fissile material as the thin reference foils in the adjacent chambers. Three DFCs containing highly-enriched ^{239}Pu (99.954%), ^{235}U (99.998%), and depleted ^{238}U (99.998%), were dedicated to the three target isotopes. The thin reference foils in each chamber are 1.27 cm diameter deposits of $\sim 10 \mu\text{g}$ ^{239}Pu and $120 \mu\text{g}$ of ^{235}U and ^{238}U while the thick activation targets are also 1.27 cm in diameter containing $\sim 220 \text{ mg}$ ^{235}U and ^{239}Pu and 440 mg of ^{238}U . A liquid scintillator based neutron detector was positioned approximately 3 m downstream of the neutron source as an additional neutron flux monitor, to measure the neutron flux fluctuation and the neutron energy spectrum in auxiliary measurements performed with pulsed proton or deuteron beams.

The absolute efficiency of the chambers used in the present measurements were found to be $100 \pm 2 \%$ using a ^{252}Cf source which is in a very good agreement with Ref.¹⁷. After irradiation, the γ -ray activity produced in the thick activation target was measured continuously for 2-3 months with well shielded and calibrated high-purity germanium (HPGe) detectors with very accurately measured efficiency. The fission products were identified from their characteristic γ -ray energies and half-lives, and their FPY were evaluated from observed photopeak areas and dual-fission chamber counts using (Eq. (1)),

$$Y_i = \frac{N_i}{N_f}, \quad (1)$$

where N_i is the number of nuclei produced during activation as determined by γ -ray counting and N_f is the total number of fissions in the activation target determined using a weighted average of the total fissions from each fission chamber and mass scaled to the thick activation target¹³. The advantage of using the DFC method is that the fission chamber determines the total number of fissions in the target without having to explicitly know either the fission cross section or the neutron flux and thus greatly reduces the total uncertainty of the measurements.

FPY measurements have been made on the three isotopes of interest at the seven incident neutron energies of 0.56, 1.37, 2.37, 3.6, 4.6, 5.5, 8.9 and 14.8 MeV. Typically, irradiation lengths ranged from 4-6 days depending on neutron flux and fission cross section. For each energy, approximately 16 cumulative FPYs were determined, nearly all being high-yield fission products, i.e., those occurring in the peaks of the mass distributions.

3. Results

The high-accuracy of the FPY measurements performed over an energy range from 0.58 to 14.8 MeV unveil a peculiar energy dependence. At low neutron energies the FPYs for asymmetric fission of ^{239}Pu and ^{238}U show a slight yield increase with increasing neutron energy from 0.5 to approximately 4-5 MeV. At $E_n > 5$ MeV the slope becomes negative for all three ^{235}U , ^{238}U , and ^{239}Pu fissile actinides. This is an important finding because it demonstrates that the high-yield fission products can have a dependence on incident neutron energy and hence has a significant impact on deduced fission yields. As an example, the experimental results from six high-yield fission fragments such as $^{95,97}\text{Zr}$, ^{99}Mo , ^{140}Ba , ^{143}Ce , and ^{147}Nd from neutron induced fission of ^{239}Pu , ^{235}U , and ^{238}U are depicted in Fig. 2. As can be seen, the FPY of ^{147}Nd (bottom right panel) shows a positive energy trend in the $E_n < 5$ MeV region. This trend is almost linear up to about 4 MeV. The relative slope of $Y(^{147}\text{Nd})/E_n = (5.6 \pm 1.6)\%/\text{MeV}$ measured from 0.58 to 3.6 MeV confirms the earlier assessment from critical assembly measurements for fission neutrons below $E_n = 2$ MeV^{3,18}. At higher energies the slope of FPY for ^{147}Nd turns over and becomes negative with relative slope of $Y(^{147}\text{Nd})/E_n = (-2.8 \pm 0.7)\%/\text{MeV}$ measured from 4.6 to 14.8 MeV. Compared to 4.6 MeV, the FPY of ^{147}Nd at $E_n = 14.8$ MeV has decreased by 71%. The real surprise is that the positive slope is observed for all other high-yield fission products from 0.58 to 3.6 MeV in $^{239}\text{Pu}(n,f)$ and $^{238}\text{U}(n,f)$. The strongest overall energy dependence was seen in neutron induced fission of ^{239}Pu , however as been mentioned above, similar positive slopes were obtained from the study of ^{238}U as well.

In case of $^{235}\text{U}(n,f)$ the energy dependency of the FPYs show constant or slightly negative slope from 0.5 to 5 MeV. The only common feature of all three fissile isotopes is the decrease of the FPY's with higher incident neutron energy ($E_n > 5$ MeV), which is probably due to an increased symmetric fission component.

The mass-chain-yield data in the neutron-induced fission of ^{239}Pu at 1.37 and 14.8 MeV obtained from the present data and those at 1.5 and 14.0 MeV from the evaluated cumulative FPYs²¹ are shown in Fig. 3. The associated figures for ^{235}U , ^{238}U , and ^{239}Pu are very similar, i.e., the fragments are formed in the well-known two-humped yield distribution, favoring an unequal division of masses. The mass-yield data show a slight increase of fission yields in the near symmetric mass region (valley) with increasing incident neutron energy in the 1.5 to 14 MeV range with only

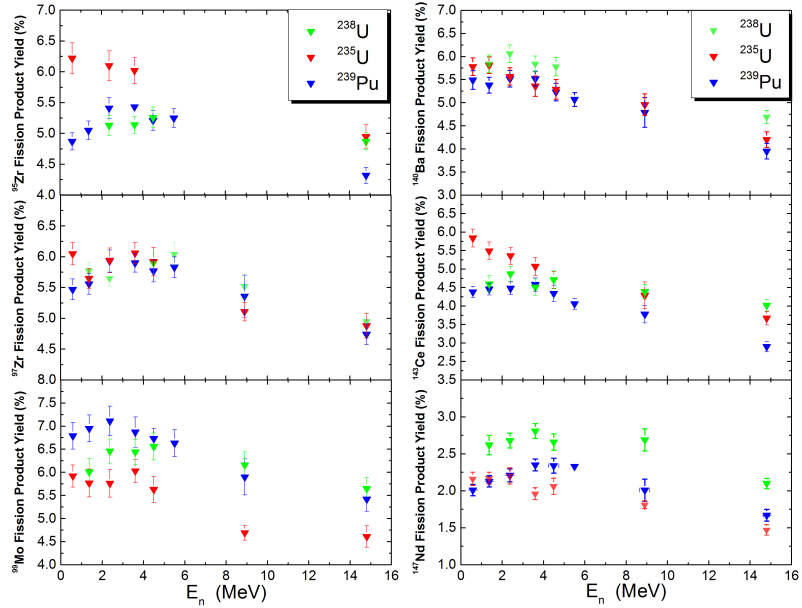


Fig. 2. (Color online) Fission product yield of ^{95}Zr (left-top), ^{97}Zr (left-center), ^{99}Mo (left-bottom), ^{140}Ba (right-top), ^{143}Ce (right-center), and ^{147}Nd (right-bottom) from the fission of ^{238}U (green triangles), ^{235}U (red triangles), and ^{239}Pu (blue triangles) in the 0.5 MeV to 15 MeV neutron energy range.

small changes in yield in other regions of the mass distribution. The increase of the symmetric FPY is accompanied by a decrease of the FPY for asymmetric fission, resulting in a substantial reduction in the peak-to-valley mass ratio with increasing neutron energy.

4. Conclusions

The unexpected trend of the FPY cannot always be reproduced by existing, data-based phenomenological models. An even larger challenge for all fundamental theory-based models of nuclear fission is the positive slope found for high-yield fission products from neutron induced fission on ^{239}Pu and to a lesser extend on ^{238}U . This is contrary to the low-energy slope of the same FPYs from ^{235}U , suggesting different interplay between the pairing and shell effects in these fissile nuclei at low-excitation energies²⁰. Therefore, the new results presented here have important applied interest for yield extraction²². The FPY increases observed at low-energies are also providing valuable fundamental new information to constrain science-based

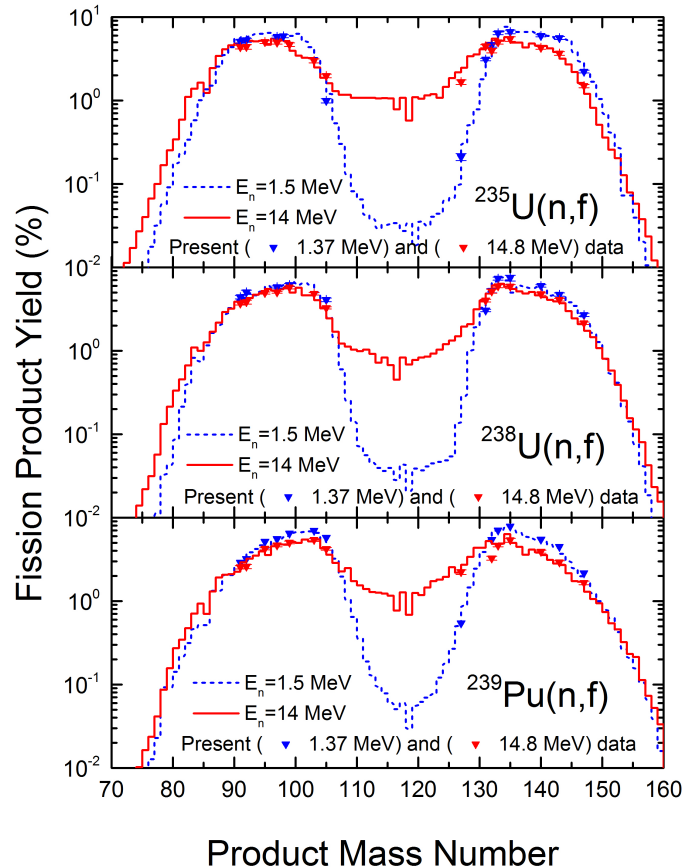


Fig. 3. (Color online) Symbols: yields of fission products (%) as a function of mass number from neutron induced fission of ^{235}U (top), ^{238}U (central), and ^{239}Pu (bottom) at 1.37 and 14.8 MeV. Curves: evaluated fission product yield distribution from fast (1.5 MeV) and high-energy (14.0 MeV) neutrons is shown in continuous lines²¹.

models of nuclei in general, and fission in particular. This study provides a rather comprehensive understanding of the FPY from the three major actinides over a wide range of fast neutron energies. Our intention is to further extend our measurements beyond the second chance fission where the energy dependency might be influenced by a complicated interaction between nuclear shape and temperature.

5. Acknowledgments

This work was performed under the auspices of US Department of Energy at Duke University and Triangle Universities and Nuclear Laboratory through NNSA, Stewardship Science Academic Alliances Program Grants No. DE-FG52-09NA29465 and No. DE-FG52-09NA29448 and at Lawrence Livermore National Laboratory operated by the Lawrence Livermore National Security, LLC under Contract No. DEAC52- 07NA27344 and at Los Alamos National Laboratory operated by the Los Alamos National Security, LLC under Contract No. DE-AC52-06NA25396.

References

1. R. Wandenbosch and J. Huizenga *Nuclear Fission* (Academic Press, Inc., New York, 1973).
2. C. Wagemans, editor *The Nuclear Fission Process* (CRC Press, Inc., Boca Raton, Florida, 1991).
3. M.B. Chadwick, et al., *Nucl. Data Sheets* **111**, 2923 (2010).
4. J. Laurec, et al., *Nucl. Data Sheets* **111**, 2965 (2010).
5. M. MacInnes, et al., *Nucl. Data Sheets* **112**, 3135 (2011).
6. D. R. Nethaway et al., *Phys. Rev. C* **16**, 1907 (1977).
7. A.C. Hayes, et al., *Phys. Rev. Lett.* **112**, 202501 (2014).
8. K-H. Schmidt, *Europhy. Lett.* **83** (2008) 32001, GEF v2.2 (2013).
9. N. Schunck, D. Duke, and H. Carr. *Phys. Rev. C* **91**, 034327 (2015).
10. J. Randrup and P. Moller, *Phys. Rev. C* **88**, 064606 (2013).
11. K-H. Schmidt, *Europhy. Lett.* **83** (2008) 32001, GEF v2.2 (2013).
12. N. Schunck, D. Duke, and H. Carr. *Phys. Rev. C* **91**, 034327 (2015).
13. M.E. Gooden, Ph.D. thesis, North Carolina State University (2014).
14. C. Bhatia, et al., *Phys. Rev. C* **91**, 064604 (2015).
15. M.E. Gooden et al., *Nucl. Data Sheets* **131**, 319 (2016).
16. C. Bhatia, et al., *Nucl. Instrum. Meth. Phys. Res. A* **757**, 7 (2014).
17. J.A. Grundl, D.M. Gilliam, N.D. Dudey and R.J. Popek, *Nucl. Tech.* **25**, 237 (1975).
18. I. Thompson, et al., *Nucl. Sci. Eng.* **171**, 85 (2012).
19. H.D. Selby, et al., *Nucl. Data Sheets* **111**, 2891 (2010).
20. N. Schunck and J. Randrup, private communication.
21. T.R. England and B.F. Rider, Los Alamos National Laboratory, LA-UR-94-3106; ENDF-349 (1993).
22. J. Lestone, *Nucl. Data Sheets* **112**, 3120 (2011).